Proceedings of the Twenty-third (2013) International Offshore and Polar Engineering **www.isope.org**
Anchorage, Alaska, USA, June 30–July 5, 2013

ISBN 978-1-880653-99–9 (Set); ISSN 1098-6189 (Set)

Modeling and Detection of Hydrodynamic Trends for Advancing Early-Tsunami Warnings

Zoheir Sabeur and Banafshe Arbab-Zavar
IT Innovation Centre, Faculty of Physical and Applied Sciences, University of Southampton
Southampton, Hampshire, United Kingdom
Joachim Wächter, Martin Hammitzsch, Peter Löwe and Matthias Lendholdt
Helmholtz-Zentrum Potsdam, Deutsches GeoForschungsZentrum, Postdam, Germany
Alberto Armigliato, Gianluca Pagnoni and Stefano Tinti
Department of Physics, University of Bologna, Italy
Rachid Omira
Department of Seismology and Geophysics, the Meteorological Institute, Lisbon, Portugal

ABSTRACT

The automated detection of tsunamigenic signals at oceanic observation stations is highly desirable for the advancement of current tsunami early warning systems. These are supported with matching methods using large numbers of tsunami wave propagation modeling scenarios. New techniques using real-time scanning of hydrodynamic signals around a network of stations in an open ocean have been developed for the detection of tsunamis. Spectral ratios with respect to background signals and their levels of similarity across stations were investigated. The new developed algorithms will be wrapped as a reporting web service for the TRIDEC tsunami early warning system in the future.

KEY WORDS: Tsunami wave propagation models; tsunamigenic signal detection; data fusion; tsunami spectral analysis; tsunami signal re-identification; TRIDEC system of systems; Open Geospatial standards.

INTRODUCTION

The rapid development of information communication and sensing technologies over the last decade has led various research programmes to be launched for building the next generation information decision-support systems which specialise in large scale environmental crises management with advanced situation awareness. In the TRIDEC research programme of Collaborative, Complex and Critical Decision-Support in Evolving Crises (Sabeur, *et al,* 2011) one focuses on the development of software architecture of open interoperable services that support the intelligent management of large volumes of data from heterogeneous sources (Moßgraber *et al,* 2012). The efficient handling of large information and heterogeneous data is of paramount importance so that key knowledge for decision support is critically extracted and delivered to decision-makers during evolving crises. Specifically, it requires the deployment of a structured framework of data fusion and modelling for the management of data and information, while overcoming their increase in volumes, heterogeneity and inherent semantic gaps. The fusion framework addresses: *a) Data semantic alignments; b) Data aggregation; c) Processing data for both tsunami wave modelling scenarios and automated detection of tsunamigenic patterns; and d) Prediction of trends with computed spatial levels of confidence*. The generated results from these respective levels of intelligent data management is stored in a Knowledge Base and made accessible on-demand under the TRIDEC system of systems (Sabeur, *et al,* 2012a). The storage solutions for the Knowledge Base are an inclusive part of the adopted intelligent information management strategies for advancing large scale decision-support systems for natural crisis management such as in TRIDEC. In this paper, a three-fold set of complementary research work conducted by the TRIDEC consortium of partners is described. It reflects upon the joint development required for building the next generation of the tsunami early warning systems. These include: *a) Databases of tsunami wave propagation model simulations; b) Automated detection of tsunamigenic signals and reporting; and c) A Knowledge Base with improved situation awareness for the TRIDEC system of Systems.*

TSUNAMI WAVE PROPAGATION MODELLING

Tsunami Generation by Earthquakes

The theory regarding tsunami generation by earthquakes is based on the hypothesis that the earthquake itself produces a significant vertical displacement of the seafloor in a very large area and in a very short time. Although horizontal displacements may provide a non-trivial contribution to tsunami generation, especially in complex-topography areas, it is believed that the largest effect on tsunami genesis is played by the vertical displacement component. Another key point regards the energy transfer from the crust to the ocean. Experiments and theory agree on the fact that, when a fluid is affected by the vertical displacement of a portion of the floor of the basin in which it is contained, the fluid reacts instantaneously with a vertical movement such that its free surface deformation resembles identically the deformation of the floor. As first approximation, it is assumed that the tsunami generation process is insensitive to the time history of the earthquake rupture, since this happens over time scales (typically few

seconds) that are much smaller than the typical periods involved in the tsunami process (several minutes to tens of minutes). This hypothesis may fail for very large magnitude earthquakes (Mw larger than 8.5 – 9.0). The earthquakes with the largest tsunamigenic potential are those that are able to produce the largest vertical displacements over large portions of the seafloor. Since both co-seismic displacements and the area affected by the deformation are increasing functions of the seismic moment (or of the magnitude), the tsunamigenic potential of an earthquake increases with the seismic moment of the earthquake. Moreover, it is straightforward that submarine earthquakes are more effective in generating tsunamis than earthquakes occurring close to the coast or inland. Furthermore, shallow-hypocenter events are more tsunamigenic than those having a deep focus. Finally, earthquakes with focal mechanisms producing prevalently vertical displacements (normal, reverse, thrust) have larger potential than those with strike-slip focal mechanisms; which typically produce predominantly horizontal deformations. Tsunami catalogues indicate that the most devastating tsunamis which occurred in history were generated in correspondence with subduction zones (Polet and Kanamori, 2000; Gusiakov, 2005), where the typical fault mechanism is thrusting and the coseismic displacements can be larger than 10 m. For instance, the 26th December 2004 (Mw=9.3) earthquake in the Indian Ocean ruptured a portion of the subduction zone offshore Sumatra longer than 1000 km. Several authors, based on different types of analyses, found that the slip on the fault was highly heterogeneous and that it was as large as, or even larger than 20 m in at least two major asperity zones (e.g. Banerjee et al., 2007). In the case of the recent 11th March 2011 Mw=9.0 Tohoku earthquake, which produced a devastating tsunami and killed around 20,000 people along the Japanese coasts, the largest coseismic slip on the fault was up to 40 m (e.g. Simons et al., 2011).

Numerical Modeling of Tsunamis

Based on the assumptions which were mentioned previously, the computation of the tsunami initial condition reduces to computing the vertical displacement of the seafloor that is induced by the earthquake. The other condition that is necessary to solve the hydrodynamics equations is the initial velocity field. Since it is assumed that the initial energy of the tsunami is purely potential, by hypothesis the initial kinetic energy is null and hence the initial velocities are also null. Consequently, in order to define the initial tsunami condition, it suffices to compute the seafloor coseismic vertical displacements, which in turn can be computed from the on-fault slip distribution using the elastic dislocation theory (e.g. Okada, 1992). The techniques and the codes used for the numerical simulation of tsunamis have made significant progress in the last years, especially due to the highly increased interest in the tsunami research field following the 2004 Indian Ocean event. The largest part of the numerical models is based on the "long wave" or "shallow water" approximation that neglects the vertical component of the water particles velocity while it considers the horizontal velocity as uniform (or averaged) along the vertical axis. In this way, the unknowns of the hydrodynamics equations reduce to three, i.e. the free surface elevation and the two horizontal velocity components. Therefore the equations to solve are, i.e. the continuity equation (or mass conservation equation) and the two equations for momentum conservation. In order to produce the results presented here, we made use of an inviscid, non-dispersive, non-linear shallow-water model implemented into a finite-differences code (UBO-TSUFD), developed and maintained by the Tsunami Research Team (TRT) at the Department of Physics and Astronomy of the University of Bologna (Italy). The code has been tested through several benchmarks and has already been employed in the study of historical and recent tsunamis (e.g. Tonini et al., 2011). The version we use solves the equations in Cartesian coordinates over a set of nested, regularly spaced grids with varying space resolution, allowing detailed results in selected areas.

Tsunami Scenarios for Portugal

The test area was on the western Iberia region; in TRIDEC, the particular interest is on the impact of tsunami scenarios along the southern coasts of Portugal. The scenario approach (see for instance Tinti and Armigliato, 2003) is one of the two main approaches traditionally used in tsunami hazard to risk assessment practices, the other one being based on probabilistic/statistical analyses. The main underlying idea is to select what is usually called a "worst-case scenario", which in turn is chosen on the basis of historical, tectonic and geological/geomorphological considerations. Following this approach, five different earthquake sources have been selected near western Iberia (Omira *et al*, 2009). Here we adopted only one of these faults, namely the Horseshoe Fault (HSF), which has been responsible for some moderate-to-large magnitude earthquakes in the recent past (28th February 1969, M_w=7.8; 12th February 2007, M_w=6.0). It has also been considered by many authors as one of the possible responsible faults for the great Lisbon earthquake which occurred on 1st November 1755 (Stich et al., 2007).

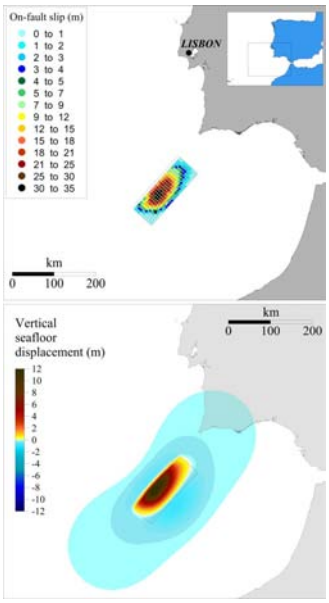

Fig.1. Upper panel: Heterogeneous slip distribution on a simplified geometry for the Horseshoe fault (HSF). Lower panel: vertical component of the seafloor displacement induced by the prescribed rupture. Positive and negative displacements indicate uplift and subsidence, respectively.

Fig. 1 shows the geometry of the fault, which is modelled as a 165 km long and 70 km wide rectangle, with pure thrust focal mechanism and dipping at 35° to the South-East. The geometry and the adopted average slip (10.7 m) are compatible with a moment magnitude M_w=8.3. The rectangle has been discretised into a matrix of 25x10 sub-faults with the aim of introducing a (purely hypothetical) heterogeneous slip distribution, whose pattern is shown in the upper panel of Fig. 1. Each subfault is characterised by a uniform slip. By means of the Okada (1992) model we computed the seafloor vertical deformation induced by the prescribed slip distribution on the fault, and resulting in the displacement field illustrated in the lower panel of Fig. 1. This coincides with the tsunami initial condition. We simulated the ensuing

tsunami by means of the UBO-TSUFD code. As mentioned earlier, the code can make use of nested grids: in this particular application, we are interested in obtaining the best spatial resolution in correspondence with five coastal places where sea-level monitoring sensors of the Portuguese network are installed. The nesting configuration, shown in the lower right panel of Fig. 2, involves a master 1-km resolution grid (the larger domain) including two 200-m resolution grids: the first covers the largest part of the Portuguese coastal area, while the second covers the Madeira island area. In turn, the first 200-m grid includes four 40-m resolution grids including the harbours of Cascais, Sesimbra, Sines and Lagos where tide gauge sensors are installed. Similarly, a 40-m grid covering the Funchal installation is nested into the second 200-m grid. Overall, 8 grids have been used for modelling the tsunami wave propagation scenarios.

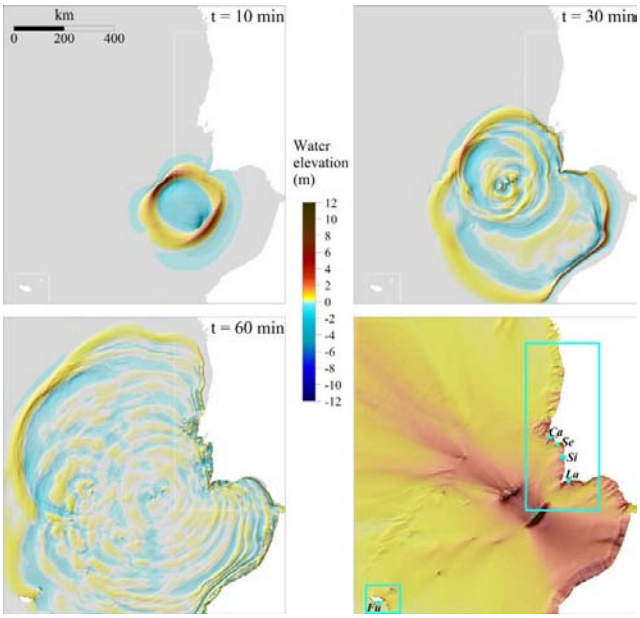

Fig.2. Tsunami propagation fields computed at 10, 30 and 60 minutes after the earthquake onset, and maximum water elevation (lower right picture) after four hours. The limits of the computational grids (cyan rectangles) have also been indicated in the lower left panel: Ca-Cascais, Se-Sesimbra, Si-Sines, La-Lagos, Fu-Funchal.

Fig. 2 shows some of the possible outputs of UBO-TSUFD. Three snapshots of the time evolution of the tsunami waves are displayed respectively at 10 min, 30 min and 1 hour after the earthquake onset, which in our approximation coincides with the tsunami generation. The pattern of propagation is rather complicated and is mainly determined by the bathymetry of the seafloor, the coastal morphology and the geometry of the fault. The latter determines the preferential direction with which the tsunami energy propagates from the source. In the HSF case which we considered, two main fronts are seen to propagate in opposite directions in the panel relative to 10 min after the tsunami generation: one towards North West and the other one towards South East. Both are almost perpendicular to the strike of the fault. In the following time frames we can appreciate the role of bathymetry and coastal morphology, which induce a number of effects on the propagating waves, including reflection, refraction and diffraction. Recalling that tsunami waves travel much faster in deep waters than in shallow waters, it is seen that, upon approaching the coastlines, the tsunami fronts tend to squeeze and to increase their amplitudes. The lower right panel of Fig. 2 shows the maximum wave elevation computed in each grid cell after four hours from the tsunami generation. The pattern of the field confirms the main observation drawn previously. The preferential direction of tsunami energy propagation is determined by the strike of the fault, while bathymetry is responsible for secondary offshore "beams" and for the distribution of the largest impacts along the coastlines.

The above modeling work represents the typical backbone approach for the development of databases with rich content of tsunamic wave propagation realisations under various types of earthquakes. These usually support the depiction of the best matching scenario of tsunami genesis under a detected earthquake event with a given epicenter location. In the next section, we present a supporting approach which specializes in the automated detection of tsunamigenic signals that are extracted from multiple observations from a network of hydrodynamic stations in an open ocean.

AUTOMATED DETECTION OF TSUNAMIGENIC SIGNALS

Regular geophysical monitoring of seismic activity at or near seas and oceans provides an opportunity for early tsunami warning by selecting from a database of pre-computed tsunami scenarios in an attempt to predict the waveform and the run-ups of the putative tsunami at potentially affected coastal zones. With current improvements in the speed of execution of these simulators, it may even be possible to use the seismic source characteristics as the input to these simulators and thus execute a more relevant simulation in real time. However, there is still another hindering factor in that it remains difficult and challenging to obtain the rupture parameters of the tsunamigenic earthquakes in real time and simulate the tsunami propagation with high accuracy. Therefore even with fast simulators a question remains on the relevance of a certain simulated tsunami signal as compared to the real hydrodynamic signal. An evaluation of the observed sea-level signal is therefore beneficial. Furthermore, in some cases the seismic signal might be absent, for example in the case of submarine landslides and volcanic eruptions which may not have been preceded by an earthquake (Gisler, 2009).

For an early tsunami warning, the analysis of sea-level data in deep waters away from the shore is required. Indeed, if the tsunami is detected at the shore, it is already too late to issue a warning. In deep waters, tsunamis propagate with modest wave heights. It is only when these waves enter shallow waters that by wave shoaling effect their wave height is increased significantly. These relatively low amplitudes of tsunami signals at deep waters along with frequent occurrence of background signals and noise contribute to a generally low signal to noise ratio for the tsunami signal; which in turn makes the detection of this signal very challenging. Tidal components account for a significant part of the hydrodynamic signal. Being deterministic in nature, they can be easily estimated and filtered out at each location of interest. There are, however, several other factors which are not as easily removable. Shelf resonance and local resonant features may also interfere with the tsunami signal (Rabinovich, 1997). Wind waves, swell and associated infra-gravity (IG) waves can create significant background noise at tsunami frequencies (Rabinovich and Stephenson, 2004). Furthermore, the tsunami wave train is constantly modified by refraction by seafloor features and reflection from continental margins.

Recently there has been an interest in automatic detection of tsunami signal from sea-level data. Simple thresholding methods have been used by Mofjeld (1997), and Rabinovich and Stephenson (2004). Artificial neural networks based applications to this problem were also

investigated by Beltrami (2008). Bressan and Tinti (2011, 2012) used the slope of sea-level signals to detect tsunami and tsunami-like signals while they designed performance indicators to evaluate the results. In these approaches, the sea-level time series signal is analyzed directly to detect the existence of tsunami or tsunami-like fluctuations.

In addition to the above, the transform of signals and the further usage of the spectral properties of signals is required. The spectral signature of a tsunamigenic signal is representative of its source event and it is preserved along its propagation path. This provides a unique opportunity to re-identify a spatially propagating tsunami from the spectral properties of the sea-level signal at different hydrodynamic stations. In this proposed approach, the following potential advantages are sought for decision-support: *a) Improvement of detection confidence; b) Increased sensitivity to weaker signals; and c) Facilitating the prediction of resonance effects at costal zones*. Nevertheless, it should be noted that by definition the methods that use the sea-level time series directly offer a more instant solution. In these, only few consecutive readings of the sea-level are used to make detections. Spectral analysis of the signals, on the other hand, requires a larger portion of observation data. While, obviously, an instant solution is desirable, the state-of-the-art instant solutions are simply impractical for detecting weaker signals in open oceans. In such cases and if the time constraints allow, a solution can be offered through automatic analysis of spectral properties and detections of tsunami signatures. A good balance can be achieved by combining the two approaches to provide both instant and more detailed detections.

Spectral Properties of Tsunamigenic Signals

It is well-known that the spectra of tsunami signals from different events recorded at the same location are similar, while the same tsunami recorded at different locations can be strongly different. This was first proposed by Omori (1902) and was later examined in many other studies (e.g. Miller, 1972, Bressan and Tinti, 2011). The properties of tsunami signals recorded at the coast are mainly determined by resonant influence of local topography rather than by the tsunami source characteristics. On the other hand, the tsunami signal at the open ocean away from the effects of the local topography is considered a valuable source for determining the source characteristics. At times, analyzing an open ocean tsunami signal can provide finer details, regarding the source event, than can be obtained from analyzing the respective seismic data.

The periods T_n of the tsunami signal are related to the dimension of the source event W and the mean water depth in the source area H, and is given by the relation:

$$T_n \sim \frac{W}{n\sqrt{gH}} \ , \ n = 1,2,...$$

where g is the acceleration due to gravity (e.g. Rabinovich, 1997). Notwithstanding the small increase in the period of tsunami wave constituents during long distance propagation (Munk, 1946), the period of the tsunami constituents can be assumed to remain invariant all along its spatial propagation path . Thus the energy spectrum pattern of the tsunami signal which is representative of its source characteristics is for the most part maintained. We will refer to this spectral pattern as the "tsunami signature". Rabinovich (1997) has shown that, even for the coastal regions, where the resonance influences of the local topography may conceal the spectral characteristics of a tsunami source, these influences can be estimated and removed, and thereby the unique spectral pattern of the tsunami can be revealed.

Detecting the Tsunamigenic Signals

Given that every tsunami signal has a signature which is representative of its source characteristics and that this signature is maintained through its propagation path, we propose a re-identification framework in which a tsunamigenic signal is detected via scanning a network of hydrodynamic stations with water levels sensing in an attempt to re-identify the same signature as the tsunami wave propagates through this network (see Sabeur *et al.*, 2012b for an earlier brief description). Thereby the probability of erroneous detections due to low signal to noise ratio is reduced and therefore higher confidence levels are achieved. As well as supporting the initial detection and improving the confidence of detection, a re-identified signal is indicative of the spatial range of the signal, and thus it can be used to facilitate the identification of certain background signals such as wind waves which generally do not have as large a spatial reach as tsunamis. This approach for signature matching can also be potentially used for a more reliable matching with a pre-computed tsunami dataset while it can also be used to predict resonance effects at the shore where the costal oscillation patterns are known, as well as providing insights as to the tsunami wave propagation path.

A scan of a set of hydrodynamic stations will be made synchronously, utilizing a set of already detected putative tsunami signal/s for the re-identification of the same tsunamigenic signal/s. In this, the Power Spectrum Density (PSD) ratio with respect to the background, as was described in (Rabinovich, 1997), is computed at each station in real-time and is firstly assessed for any significant oscillations that are different from the background and further compared against the putative tsunami signature/s which have been previously detected at any of these stations in an attempt to re-identify a propagating tsunami wave. To obtain the PSD ratio of a segment of the hydrodynamic signal, the tidal components of the signal are first removed using the previously estimated tidal components at that location and the signal is also de-trended. The spectral ratio is computed by taking the ratios of the PSD values of this signal and the background signal at the corresponding frequencies. When analyzing the spectral ratio of the current segment at a station, two main questions are asked: i) Does the signal include any oscillations which are significantly different from the background? ii) Does the signal have a spectral signature similar to any of the previously detected signatures? If both answers are positive a strong re-identification has been made. If the signal is significantly different from the background but does not resemble anything that was observed before, this is considered a new signature and a new putative tsunami. This is certainly the case when we first start scanning since there are no prior detections. Finally, a signal which is weak but has a signature similar to what has been seen before presents one of the main cases for which the proposed re-identification framework can be very beneficial where a weak signal which would not have been otherwise detected is identified.

Experiments

In our initial test, we have investigated a set of deep-ocean bottom pressure gauges (BPR) in the Pacific Ocean for the Chilean tsunami of 27th of February 2010. This data is provided by the Deep-ocean Assessment and Reporting of Tsunamis (DART) buoys network system of the National Oceanic and Atmospheric Administration (NOAA) (González et al., 1998). This tsunami was generated by an $M_w = 8.8$ earthquake off the Southern coast of Chile and was observed across the Pacific Ocean. We have scanned five DART stations: 21413 (North West Pacific), 21414 (North Pacific), 51406 (Central Pacific), 51425 and 51426 (west Pacific). Fig. 3a shows the location of these stations in the Pacific Ocean. We assume that we can receive the sea-

level readings from these stations in real-time. Clearly, at each station the tsunami can be only observed when and if it arrives at that station. Note that in order to be able to calculate spectral ratios we need to have knowledge of the background oscillations at each station. Therefore a Δt time, which we refer to as the initialization time, in the beginning of each observation is devoted to capturing the characteristics of the background signal. Once this is performed we can proceed with the scan phase. In a mock real-time scan of these stations. A record of each detected putative tsunami signal which has been observed at any one of these stations is retained and used as the reference list for the re-identification purpose. Spectral ratios are compared using the Manhattan distance of normalized spectral ratios. Normalization is achieved using the decibel unit and the maximum PSD ratio value for each signal as the reference value, to ensure that the signals are compared based on their energy distribution rather than their energy levels. Two threshold values are used: one to determine whether the signal is significantly different from the background, and the other to determine a match between the currently analyzed spectral ratio and previously detected signature/s. For multiple detections of a signal the mean spectral ratio is used as the signature for that detection.

The sampling frequency of these stations is 15 seconds. We analyze 12.8 hours segments of sea-level data at each step. This analysis is repeated every 15 minutes, thus a sliding window with a 15 minutes step size is used (Fig. 3b.). The computation time required to analyze one segment at one station is of an order of deciseconds with an Intel(R) Core(TM) i7-2600 CPU @ 3.40GHz processor and 16GB of RAM. The first 12.8 hours segment is used for the computation of background PSDs. We start our scan at zero hour of the 23rd of February 2010 and finish at midnight on 5th of March 2010.. Fig. 4 shows the spectral ratios (the tsunami signature) for this tsunami detected automatically at the five stations using the method described above. The detected spectral ratios present a trend in the spectral distribution of energy for this tsunami which can be seen more clearly in the grey graph line, which is the mean value of the detected signatures. As well as the general trend which is similar between the spectral ratios detected at different stations, the mean signal has dominant peaks at periods 32 min, 14 min and 7 min. The two smaller periods are in good agreement with the Rabinovich et al. (2012) work which have reported dominant periods of 6-8 min and 15 min for this tsunami from six deep-sea observations by BPRs located seaward from the coasts of Vancouver Island and Washington State.

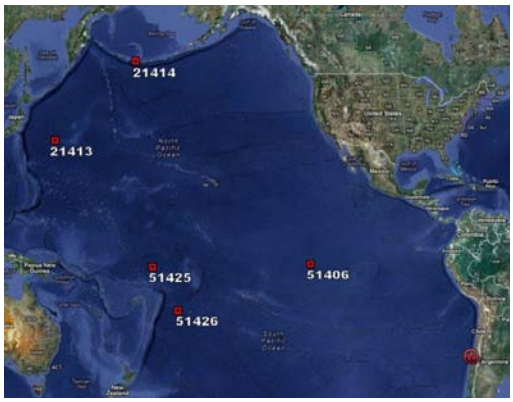

Fig.3a. DART stations and the epicenter of the 2010 Chilean tsunami.

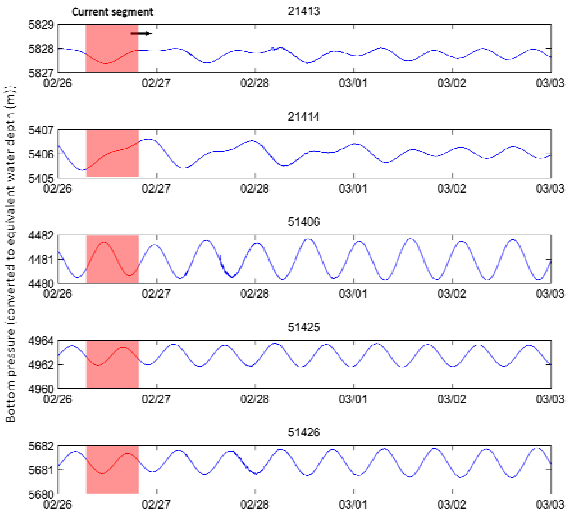

Fig.3b. Synchronous scan of the five DART stations

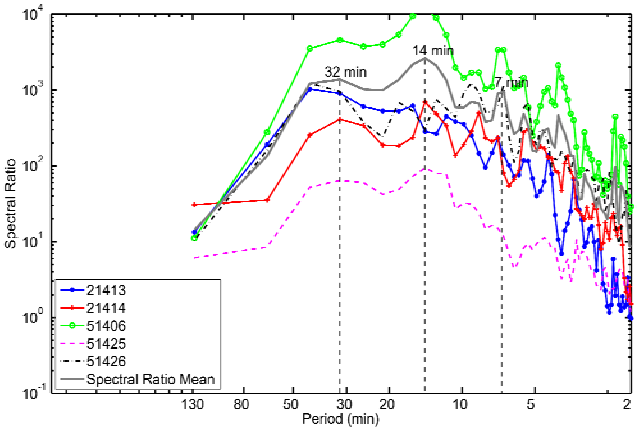

Fig.4. The spectral ratio of the 2010 Chilean tsunami automatically detected on five DART stations demonstrates a good similarity between the spectral ratios at different stations.

The main detected matching signatures that are shown in Fig. 4 are one of three signature sets that are detected during our 11 day scan of the five DART stations, and it represents the most energetic signal. The two other detected signatures one corresponds to seismic waves which are generally characterized by a higher frequency profile and the other to the tail of the tsunami signal. As the tsunami wave propagates it becomes increasingly more complex due to various refractions and reflections thus other patterns start to emerge. However, these signals are generally less energetic than the initial tsunami wave.

In the next section, the TRIDEC tsunami early warning system is introduced. While, it currently uses the matching scenario approach for tsunami warning, it shall be further advanced with supporting new intelligent information management modules under the TRIDEC project. Among these new modules will be an alert service for automated detection of tsunamigenic signatures, which is based on the technique of signal analysis described above.

TRIDEC TSUNAMI EARLY WARNING SYSTEM

Following the Boxing Day Tsunami of 2004, research initially addressed isolated activities to improve Tsunami Early Warning (TEW) capabilities. Over time, the focus changed towards the establishment of reference architectures using standardised interfaces and reusable components. This allowed the porting of complete TEW systems (TEWS) or components to other regions of the world or application for natural crises in general (Wächter et al., 2012).

Within a standards-based TEWS, a situation picture component, provided via a Graphical User Interface (GUI) serves as the central point of information for the Officers on Duty (OOD) to guide them through the TEWS workflow (Fig. 5). The situation picture is based on spatial data such as thematic maps and sensor observations. Spatial data are provided via Open Geospatial Consortium (OGC) Web Map Service (WMS) and the OGC Web Feature Service (WFS). Tsunami simulation information can also be accessed using a OGC Web Processing Service (WPS) (Hammitzsch et al., 2012).

TEWS use incoming sensor data to predict the expected tsunami propagation pattern for the current event. This prediction is used to identify regions and critical infrastructure under threat. In the following, information logistics components compose and distribute warning messages for selected recipients like government agencies, which will disseminate the information further towards the affected communities.

Fig.5. Simplified workflow of a Tsunami EarlyWarning System (Lendholt and Hammitzsch, 2011).

Tsunami Simulation

A core concept for Tsunami Early Warning Systems is the use of Tsunami simulation products, based on bathymetry, topography and incoming sensor observations. These parameters are used to infer the likely Tsunami spreading origins, to predict the propagation pattern and the overall spatial and temporal extent of the Tsunami.

Simulation products are based on point grids, with wide mesh sizes in the open sea and decreasing mesh sizes closer to the shorelines. The simulation results are three-dimensional data sets, which factor in local tides to state expected water level deviations.

An important part of the Tsunami propagation prediction is the estimate of arrival times and expected wave heights for affected coastal areas (Behrens et al., 2010). Models, algorithms and software systems used to produce Tsunami simulation products are a focus of current research.

Visualizing Tsunami Parameters

Previous research activities in the projects *German Indonesian Tsunami Early Warning System* (GITEWS, www.gitews.de), *Distant Early Warning System* (DEWS, www.dews-online.org) and *Collaborative, Complex and Critical Decision-Support in Evolving Crises* (TRIDEC, www.tridec-online.eu) identified the following simulation products as suitable for visualization in a TEWS workflow:

(i) Maximum water levels show maximum wave heights at selected locations within a defined observation timeframe (Fig. 6).

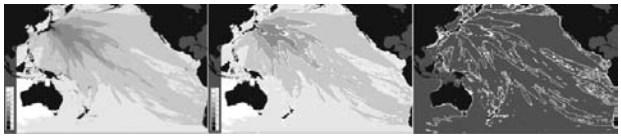

Fig. 6. Simulated maximum Tsunami water levels are mapped as discrete grey levels (left), combined with isolines (centre) and solely as isolines (right). (Lendholt et al., 2012).

(ii) Isochrones map the advancing of the Tsunami wave front. This can be combined with other information, including maximum water levels (Fig. 7). Since isochrones can be derived for various parameters, the observed variable has to be explicitly stated (e.g. first wave front or other).

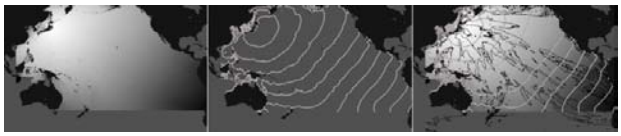

Fig.7. *Isochrones* for the estimated arrival time (ETA) of a Tsunami simulation shown as continuous grey values (left), as isolines (center) and as a composite (right), consiting of isochrones (light grey), isohypses (black) and ETA-isochrones. (Lendholt et al., 2012).

(iii) Mareograms show sea level time-series for selected locations, e.g. tide gauge sensor positions (Fig. 8). Combined with incoming observation data mareograms can be used to manually assess simulation validity and information value.

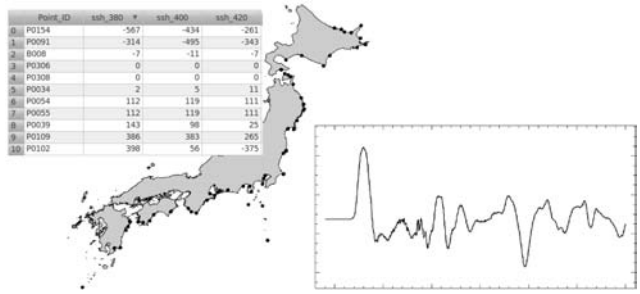

Fig.8. *Mareograms* for selected coastal locations of the Japanese coast displaying water level changes over time, shown as a table (top left) and plot (bottom right). (Lendholt et al., 2012).

(iv) Worst-Case-Estimates contain coastal forecasts for selected locations including the Estimated Time of Arrival (ETA) of the Tsunami wave fronts and maximum Estimated Wave Heights (EWH). This information allows for a simplistic yet effective threat classification for affected coastal regions (Lendholt, 2011). All four described visualisation products are accessed as vector data in the TEWS environment, having been derived from raster-based simulation data sets. They are complemented by a non-vector product.

(v) Tsunami-animations are used as dynamic overlays for static maps to foster intuitive understanding of the spatio-temporal dynamics of the Tsunami event. Within the TEWS workflow they are used for high-level overviews of reduced spatial resolution or to show local effects within a limited time interval. An alternative application is visual quality assessments of Tsunami simulations, to ensure their spatial and temporal consistency and validity. Within TRIDEC, several workflows have been set up to generate animation products, including the GFZ

High Performance Compute (HPC) Cluster and GRASS GIS (Löwe et al., 2011 and Löwe et al., 2012).

CONCLUSIONS

The collaborative research and development work which has been pursued in the TRIDEC Integrated Project since September 2010 is converging towards building the next generation of advanced and integrated tsunami early warning system of systems. The scalable TRIDEC architecture of open processing services and a rich database of tsunami wave propagation realizations are being built for the Mediterranean and North-East Atlantic zone. Furthermore, a powerful approach based on continuous spatial scanning water level signals at hydrodynamic stations using wave spectra analyses has been successfully developed for the automated detection of tsunamis. This has the potential of providing increased situation awareness with more detailed reporting about the tsunami wave propagation in real-time and storage in the TRIDEC Knowledge Base. Also, the use open standards in the construction of the Tsunami early warning system components gives it a great potential of interoperability and low cost for coupling it with other existing early warning systems which operate in many other parts of the world oceans.

ACKNOWLEDGEMENTS

This research work is supported by the European Commission under the TRIDEC Integrated Project contract Number: FP7 258723. Also, the contributing Authors from the University of Southampton IT Innovation Centre are very grateful to NOAA for using their open hydrodynamic observation data of the Pacific Ocean, in order to achieve their development of the automated detection algorithms on tsunamigenic signals in the TRIDEC project.

REFERENCES

Banerjee, P, Pollitz, F, Nagarajan, B, and Burgmann, R (2007). "Coseismic slip distributions of the 26 December 2004 Sumatra-Andaman and 28 March 2005 Nias earthquakes from GPS static offsets," *Bull Seism Soc Am*, Vol 87, Suppl S, pp S86-S102, Part a.

Behrens, J, Androsov, A, Babeyko, AY, Harig, S, Klaschka, F Und Mentrup, L (2010). "A new multi-sensor approach to simulation assisted tsunami early warning," *Natural Hazards and Earth System Sciences*, 10, 1085 1100, Copernicus Publications.

Beltrami, GM (2008). "An ANN algorithm for automatic, real-time tsunami detection in deep-sea level measurements." *Ocean Engineering*, Vol 35, No 5, pp 572-587.

Bressan L., Tinti S (2011). "Structure and performance of a real-time algorithm to detect tsunami or tsunami-like alert conditions based on sea-level record analysis," *Natural Hazards and Earth System Sciences*, Vol 11, pp 1499-1521.

Bressan L., Tinti S (2012). "Detecting the 11 March 2011 Tohoku tsunami arrival on sea-level records in the Pacific Ocean: application and performance of the Tsunami Early Detection algorithm (TEDA)," *Natural Hazards and Earth System Sciences*, Vol 12, pp 1583-1606.

Gisler, GR (2009). "Tsunami generation: Other sources." *The Sea: Tsunamis* Vol 15, pp 179-200.

González, FI, Milburn, HB, Bernard, EN, Newman, J (1998). "Deep-ocean Assessment and Reporting of Tsunamis (DART): Brief Overview and Status Report." *Proceedings of the International Workshop on Tsunami Disaster Mitigation*, Tokyo, Japan, pp 118-129.

Gusiakov, K (2005). "Tsunami generation potential of different tsunamigenic regions in the Pacific," *Mar Geol*, Vol 215, pp 3-9.

Hammitzsch, M, Reißland, S und Lendholt, M (2012). "A Walk through TRIDEC's intermediate Tsunami Early Warning System," *Geophysical Research Abstracts*, Vol 14, Egu2012-12250.

Lendholt, M, Hammitzsch, M, Löwe, P (2012). "Harmonisierung Von Datenformaten Für Tsunami-Simulationsprodukte," *Angewandte Geoinformatik* 2012, Wichmann.

Lendholt, M (2011). "Tailoring spatial reference in early warning systems to administrative units," *Earth Science Informatics*, Vol 4, No 1, pp 7-16, Springer.

Lendholt, M und Hammitzsch, M (2011). "Addressing administrative units in international tsunami early warning systems: shortcomings in international geocode standards," *International Journal of Digital Earth.*

Löwe, P, Hammitzsch, M, Wächter, J (2011). "The TRIDEC Project: Future-Saving FOSS GIS Applications for Tsunami Early Warning," *AGU* 2011, San Francisco.

Löwe, P, Klump, J, Thaler, J (2012). "Die FOSSGIS Workbench des GFZ Compute Clusters," *Angewandte Geoinformatik* 2012, Wichmann.

Miller, GR (1972). "Relative spectra of tsunamis," *Hawaii Institute of Geophysics (HIG)* Vol 72, no. 8.

Moßgraber, J, Middleton, S, Hammitzsch, M and Poslad, S. (2012). "A Distributed Architecture for Tsunami Early Warning and Collaborative Decision-support in Crises". *Geophysical Research Abstracts,* Vol 14, EGU2012-8040-2, 2012, EGU General Assembly 2012.

Mofjeld, HO (1997). "Tsunami Detection Algorithm," *National Oceanic and Atmospheric Administration (NOAA), unpublished notes*, http://www.pmel.noaa.gov/tsunami/tda_documentation.html.

Munk, WH (1946). "Increase in the period of waves traveling over large distances : with applications to tsunamis, swell, and seismic surface waves." *PhD thesis. Los Angeles: University of California*.

Okada, Y (1992). "Internal deformation due to shear and tensile faults in a half-space," *Bull.Seism. Soc. Am.*, Vol 82, pp 1018-1040.

Omira, R, Baptista, MA, Matias, L, Miranda, JM, Catita, C, Carrilho, F, and Toto, E (2009). "Design of a sea-level tsunami detection network for the Gulf of Cadiz," *Nat Haz Earth Syst Sci*, Vol 9, pp 1327-1338.

Omori, F (1902). "On tsunamis around Japan (in Japanese)." *Rep. Imp. Earthquake Comm.*, Vol 34, pp 5-79.

Polet, J, and Kanamori, H (2000). "Shallow subduction zone earthquakes and their tsunamigenic potential," *Geophys J Int*, Vol 142, pp 684-702.

Rabinovich, AB (1997). "Spectral analysis of tsunami waves: Separation of source and topography effects." *Journal of Geophysical Research*, Vol 102, No C6, pp 12663 - 12676.

Rabinovich, AB, Stephenson, FE (2004). "Longwave Measurements for the Coast of British Columbia and Improvements to the Tsunami Warning Capability," *Natural Hazards,* Vol 32, No 3, pp 313–343.

Rabinovich, AB, Thomson, RE, Fine, IV (2012). "The 2010 Chilean tsunami off the west coast of Canada and the northwest coast of the United States." *Pure and Applied Geophysics*, pp 1-37.

Sabeur, Z, Wächter, J, Küppers, A, and Watson, K (2011). "Large Environmental Sensor Observation Data and Knowledge Base for Collaborative Decision-support in Crises". *Geophysical Research Abstracts* Vol 13, EGU2011-12300, 2011, EGU General Assembly 2011.

Sabeur, Z, Wächter, J, Middleton, S, Zlatev, Z, Rainer, R, Hammitzsch, M, and Löwe, P (2012a). " Knowledge Base and Sensor Bus Messaging service Architecture for Critical Tsunami warning and Decision-Support". *Geophysical Research Abstracts* Vol 14, EGU2012-12265, 2012, EGU General Assembly 2012.

Sabeur, Z, Arbab-Zavar, B, Samperio, R, Armigliato, A, Omira, R, Wächter, J, and Tinti, S (2012b). "Automated Detection of Tsunamigenic Signatures and Reporting Using Multi-scale offshore

in situ measurements for early Tsunami Warning and Critical Decision-support". *Geophysical Research Abstracts* Vol 14, EGU2012-12411, 2012, EGU General Assembly 2012.

Simons, M, Minson, SE, Sladen, A, Ortega, F, Jiang, J, Owen, SE, Meng, L, Ampuero, J-P, Wei, S, Chu, R, Helmberger, DV, Kanamori, H, Hetland, E, Moore, AW, and Webb, FH (2011). "The 2011 magnitude 9.0 Tohoku-Oki earthquake: mosaicking the megathrust from seconds to centuries," *Science*, Vol 332, pp 1421-1425.

Stich, D, Mancilla, FdL, Pondrelli, S, and Morales, J (2007). "Source analysis of the February 12th 2007, M_w 6.0 Horseshoe earthquake: implications for the 1755 Lisbon earthquake," *Geophys Res Lett*, Vol 34, L12308, doi:10.1029/2007GL030012.

Tinti, S, and Armigliato, A (2003). "The use of scenarios to evaluate the tsunami impact in southern Italy," *Mar Geol*, Vol 199, pp 221-243.

Tonini, R, Armigliato, A, Pagnoni, G, Zaniboni, F, and Tinti, S (2011). "Tsunami hazard for the city of Catania, eastern Sicily, Italy, assessed by means of Worst-case Credible Tsunami Scenario Analysis (WCTSA)," *Nat Haz Earth Syst Sci*, Vol 11, pp 1217-1232.

Wächter, J, Babeyko, A, Fleischer, J, Häner, R, Hammitzsch, M, Kloth, A und Lendholt, M (2012). "Development of Tsunami Early Warning Systems And Future Challenges." *Natural Hazards and Earth System Sciences*, Veröffentlichung steht bevor.